Construction and Building Materials 354 (2022) 129185

Contents lists available at ScienceDirect

Construction and Building Materials

journal homepage: www.elsevier.com/locate/conbuildmat

A bio-inspired, plant-derived admixture for metakaolin blended cement mortars

Xin Qian [a], Mengxiao Li [a], Jialai Wang [b,*], Liang Wang [b,c], Peiyuan Chen [c], Yi Fang [b,*], Xiaodong Wang [b], Fan Yang [a]

[a] Key Laboratory of Infrastructure Durability and Operation Safety in Airfield of CAAC, Tongji University, Shanghai 201804, PR China
[b] Department of Civil, Construction, and Environmental Engineering, The University of Alabama, Tuscaloosa, AL 35487, USA
[c] School of Civil Engineering and Architecture, Anhui University of Science and Technology, Huainan, Anhui 232001, PR China

ARTICLE INFO

Keywords:
Metakaolin
Dispersion
Tannic acid
Compressive strength
Bio-inspiration

ABSTRACT

Partially replacing ordinary Portland cement (OPC) with metakaolin (MK) can refine the pore structure, improve mechanical properties, and enhance the durability of concretes. However, MK tends to agglomerate due to its high surface area and high concentration of hydroxyl groups. To overcome this problem, this study exploits a plant-derived polyphenol, tannic acid (TA), as an eco-friendly admixture to disperse MK. Due to its similar chemical functional groups as the adhesive protein in the mussel byssus, TA can adhere to various surfaces like the mussel's adhesive protein. An experimental program was carried out to characterize the TA treated MK and investigate the effects of the proposed method on the properties of the cement paste and mortar. After mixing with the MK, TA can be adsorbed on the surface of MK particles, achieving deflocculation and dispersion of mineral grains by electrostatic repulsion forces and steric effect, significantly improving the workability of the mortar. Pore structure analysis suggests that TA dispersion densifies the hydration products, as revealed by the much-reduced gel and interhydrate pores. The nanoindentation results indicated that all low-density calcium hydrate silicate (C—S—H) was converted to high density by the TA dispersion, leading to a drastic improvement in the compressive strength of the produced mortars. As a result, the 28 days compressive strength of cement mortar prepared with TA dispersed MK was enhanced by up to 97 % compared with the one prepared without MK substitution, which exhibits great potential in reducing the carbon footprint of cement-based construction materials.

1. Introduction

Supplementary cementitious materials (SCMs), such as silica fume, metakaolin, and slag [1,2], are commonly used to partially replace cement, resulting in less use of cement clinker. Among these SCMs, metakaolin (MK) with very high pozzolanic reactivity appears to have great potential for the production of high-strength, and high-performance concretes. The temperature of producing MK (600–900 °C) is much lower than that of the cement clinker, and the calcination process releases much less carbon dioxide [3,4]. Both the mechanical properties and durability of the produced concrete can be significantly improved by using MK because of two primary mechanisms: 1) more calcium silicate hydrate (C—S—H)/Calcium Alumina Silicate Hydrate (C-A—S—H) is produced through the pozzolanic reaction between the calcium hydroxide (CH) and the MK; 2) the microstructure of the produced concrete is densified by the filler effect of the small particle size (~1–2 μm) of MK [5–7]. The consumption of CH, which provides minimal bonding strength in OPC-based concrete, also improved the stability and mechanical strength of the produced concrete, leading to more efficient use of the clinker.

The use of MK can also significantly improve the durability of the produced cementitious materials, such as impermeability [8], sulfate resistance [9], and freeze-thaw resistance [10]. Al-Akhras compared the sulfate resistance of cement concrete with 5 % to 15 % MK replacement and discovered that sulfate resistance increased with increasing the MK replacement level [9]. Because MK tends to agglomerate due to its high surface area and high concentration of hydroxyl groups [11], adding more MK can reduce fluidity in pastes, mortars, and concrete, significantly reducing the effectiveness of MK in concrete. Therefore, it is necessary to disperse MK to achieve better performance of the produced

* Corresponding authors.
E-mail addresses: jwang@eng.ua.edu (J. Wang), yfang20@crimson.ua.edu (Y. Fang).

https://doi.org/10.1016/j.conbuildmat.2022.129185
Received 27 May 2022; Received in revised form 9 September 2022; Accepted 12 September 2022
Available online 19 September 2022

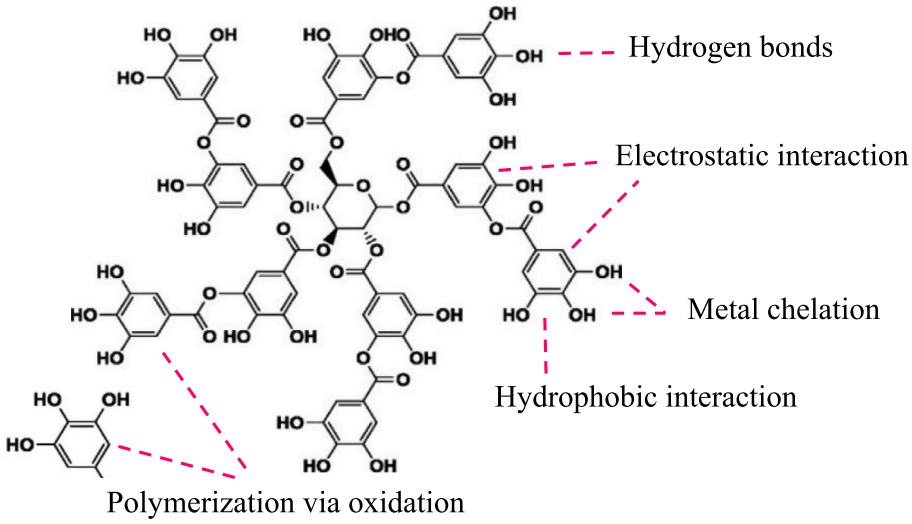

Fig. 1. Chemical structure of tannic acid.

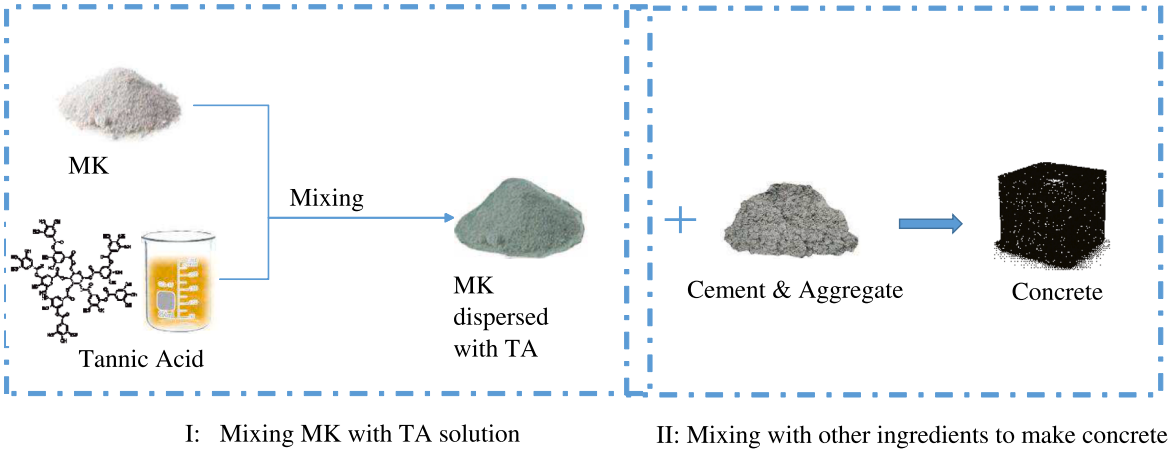

Fig. 2. Manufacturing high-performance concrete with MK dispersed by TA.

concrete. To this end, a high-range water reducer or a superplasticizer is commonly used when a higher MK replacement level is adopted [11,12]. Similar to many other commonly used chemical admixtures for concretes, however, the superplasticizer is petroleum-based. Its manufacturing and degradation can produce products detrimental to the environment.

This study proposes a plant-derived polyphenol, tannic acid (TA), as an eco-friendly polyphenol to replace the traditional water reducer for MK dispersion in concrete. TA, written as $C_{76}H_{52}O_{46}$ (Fig. 1), is the world's third-largest class of plant components after cellulose and lignin [13]. It can be extracted from plants, microorganisms [14], or decomposing organic matter in water [15] and enjoys many advantages, such as being abundant, renewable, safe, non-toxic, and cost-effective [16].

The use of TA in concrete is inspired by mussels, which display an extraordinary ability to adhere to substrates underwater [17] using adhesive proteins [18] L-3,4-dihydroxyphenylalanine (DOPA) in the mussel byssus. Waite and Tanzer [19] found that catechols of the DOPA are responsible for the versatile adhesion of mussels. Inspired by this finding and outstanding adhesion brought about by catecholic compounds, great efforts have been made to exploit catechols as the binding agent for enhancing adhesion in synthetic materials [19–22]. TA, as a plant polyphenol, also has high catechol content and, therefore, should possess a similar ability as DOPA to strongly bind to surfaces through various interactions, including coordination bond, hydrophobic interaction, and hydrogen bond with diverse functional groups [23], as shown in Fig. 1. These strong interface interactions make TA tightly bound to the surface of the nanofiller to improve the stability and prevent the aggregation or agglomeration of the nanofillers. This has been confirmed by a recent study [24], in which TA was used to successfully disperse silica nanoparticles in a silica fume blended cement mortar. Significant enhancement in the performance of produced concrete, such as workability, mechanical properties, and durability, can be achieved by the TA dispersion [24]. More importantly, TA can react with cement to produce nanoparticles in-situ [25] that are well-dispersed in the slurry due to the steric impulsion generated by π-π stacking and function in the same way as externally added nanoparticles to enhance the performance of the produced concretes.

Inspired by these successes, this study hypothesizes that TA can be used to disperse MK to achieve significant improvement in the performance of the produced mortars/concretes. To this end, a simple two-step mixing approach is adopted, as shown in Fig. 2. In the first step, MK fine particles are mixed with a TA solution. A layer of TA can be immediately adopted onto the MK particle due to the covalent and non-covalent interaction provided by the abundant terminal phenolic hydroxyl groups of TA [26]. The produced MK slurry containing TA dispersed MK particles, and residual free TA was then added to other ingredients to make concrete in the second step, as shown in Fig. 2.

To test this hypothesis, an experimental program was carried out to

Table 1
Chemical compositions of OPC and MK used in this study (%).

Oxide Composition (%)	SiO_2	CaO	Al_2O_3	Fe_2O_3	MgO	Na_2O	K_2O	LOI
Type I/II OPC	22.9	64.0	4.7	2.4	3.4	0.2	0.7	0.8
MK	59.4	0.1	30.8	1.4	2.2	2.7	1.3	0.7

examine the effects of TA dispersion of MK on the performance of MK blended cement paste/mortars. The underlying mechanisms were investigated by using X-ray powder diffraction analysis (XRD), scanning electron microscope (SEM), mercury intrusion porosimetry (MIP), and nanomechanical properties testing.

2. Materials and methods

2.1. Materials

The chemical compositions of type I/II OPC and MK were measured by X-ray fluorescence (XRF), as shown in Table 1. The median diameter (D_{50}) of the cement and MK is 15.37 μm and 3 μm, respectively, and more than 99 % of MK has a particle size of less than 16 μm. The TA used in this study is an analytical reagent with a purity of 98 %. Natural river sand was chosen as fine aggregate in this research, and its specific gravity and water absorption are 2.70 and 0.95 %, respectively. This river sand has a fineness modulus of 2.83. Before manufacturing the mortar samples, the fine aggregate and MK were oven-dried for 12 h at 110 °C.

2.2. Characterization of TA dispersed MK

The oven-dried MK was dispersed through soaking in the TA solution with solid to liquid ratio of 0.3 kg/L at room temperature of 23 °C. The concentration of TA used to make the solution was chosen as 1.3 % by the weight of the MK. After 15 min of magnet stirring, the TA mixed MK slurry was then dried at 60 °C in an oven for 24 h before characterization. Another sample was also prepared with the same procedure but soaked in deionized water for comparison purposes. The morphologies of the MK before and after TA dispersion were examined by a scanning electron microscope (SEM). The specific surface areas of the MK were measured based on Brunauer – Emmett – Teller (BET) method. The zeta potential tests were also carried out to investigate the potential stability of the MK suspensions with and without TA dispersion. X-ray diffraction (XRD) and Fourier Transform Infrared Spectroscopy (FT-IR) were also employed to examine the interaction between the TA and MK.

2.3. Setting time and flowability

Vicat needle test was employed to investigate the effect of TA dispersion of the MK on the setting time of produced blended cement paste according to ASTM C191 [27]. Five groups of paste samples with water to binder ratio of 0.3 were prepared: the control group without MK substitution, the 15MK group with 15 % MK substitution, and three groups with 15 % MK substitution dispersed by TA. The dosages of TA used for dispersing MK were 2 ‰, 4 ‰, and 6 ‰ by the weight of the total cementitious materials labeled as 15MK2TA, 15MK4TA, and 15MK6TA, respectively.

Table 2
Mix design for cement mortars produced with/without MK (kg/m^3).

Groups	Cement	MK	Water	River Sand	TA	SP
Control	360.2		180.1	907.7	–	–
15MK	306.2	54.0	180.1	907.7	–	–
15MK2SP	360.2	54.0	180.1	907.7	–	0.72
15MK2TA	356.6	54.0	180.1	907.7	0.72	–
15MK4TA	349.4	54.0	180.1	907.7	1.44	–
15MK6TA	360.2	54.0	180.1	907.7	1.44	–
10MK	324.2	36.0	180.1	907.7	2.16	–
10MK2TA	324.2	36.0	180.1	907.7	0.72	–
20MK	288.2	72.0	180.1	907.7	–	–
20MK2TA	288.2	72.0	180.1	907.7	1.44	–

Five groups of mortar samples were prepared to investigate the effect of TA dispersion on the flowability of the produced mortars by the flow table test based on ASTM C1437 [28]. The control group was made using water to binder ratio of 0.5. The 15MK group was prepared with the same mix as the control one, except that 15 % cement was replaced by the MK. Three more groups of MK blended cement mortar samples were prepared with TA dispersed MK with the same dosage of TA used in the setting time test and labeled as 15MK2TA, 15MK4TA, and 15MK6TA.

2.4. Hydration heat

The effect of TA dispersion on the hydration of the blended cement paste was investigated by using an isothermal calorimetry test based on ASTM C1679 and ASTM C1702 [29,30]. A total of five groups of paste samples were prepared with water to binder ratio of 0.5. These groups were produced by employing the same ratio between cement, MK, and TA as those in the flowability test, and these groups were also named in the same way.

2.5. Hydration products

XRD was employed to evaluate the effect of TA dispersion on the cement hydration products. The samples were obtained from the calorimetry test and stored in sealed bags to avoid contamination until the testing date. At 3 days and 28 days, the specimens were pulverized in a sealed bag. The produced cement pastes powders with a size smaller than 0.15 mm were used.

2.6. Microstructure

Two groups of cement pastes with water to binder ratio of 0.5 were prepared for the microstructure analysis. The 15MK group was prepared with 15 % pristine MK substitution. The other group, 15MK2TA, was prepared with TA dispersed MK to replace 15 % of the OPC. The dosage of TA is 2 ‰ by the weight of the total cementitious materials. Both groups were kept in a sealed plastic bag for 28 days and then examined by SEM on the microstructure and morphology of the hydration products. Before being placed in the SEM chamber, all the samples were coated with gold (Au) to prevent electron charging. Their porosities and pore size distributions were further determined using mercury intrusion porosimetry (MIP). One extra group was also prepared with the MK dispersed by 2 ‰ of superplasticizer (PCE), designated as 15MK2SP for the MIP analysis.

Nanoindentation testing was carried out to examine the effect of the proposed TA dispersion on the mechanical properties of the hydration products. To this end, paste samples were first cut to fit the 32.5 mm diameter capsule filled with epoxy resin. Then, the specimens were taken out and polished with 240, 600, 800, and 1200 grit silicon carbide sandpaper followed by 3 μm diamond suspension, 1 μm diamond suspension, 0.3 μm alumina suspension, and 0.05 μm alumina suspension on a felt pad. A nanoindenter was employed to conduct a grid of 20*20 nanoindentations with 10 μm spacing on the prepared specimens. During the indentation process, the load was increased linearly to 1mN with multiple partial unloading, then held constant for 2 s, and finally decreased linearly back to zero in 5 s. The unloading recordings between

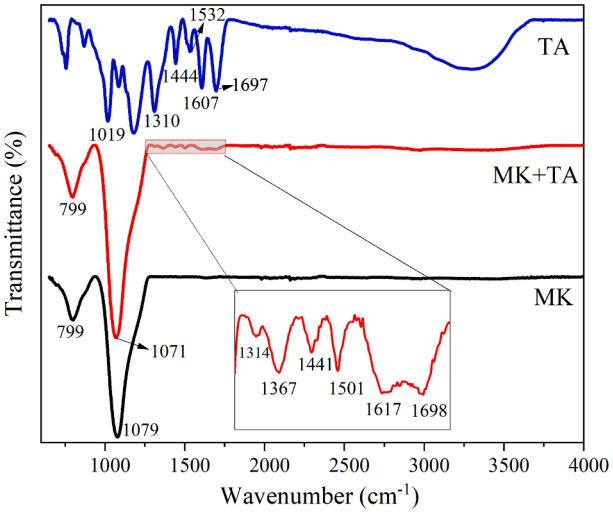

(a)

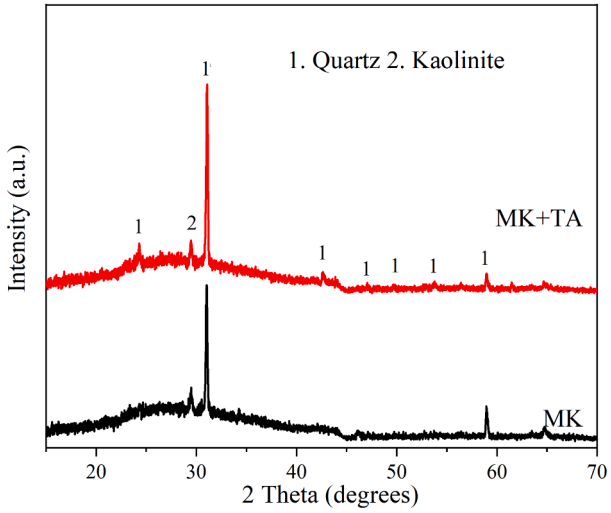

(b)

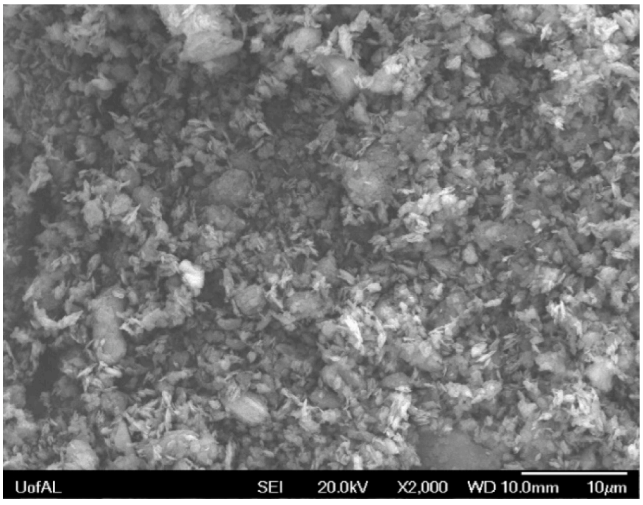

(c)

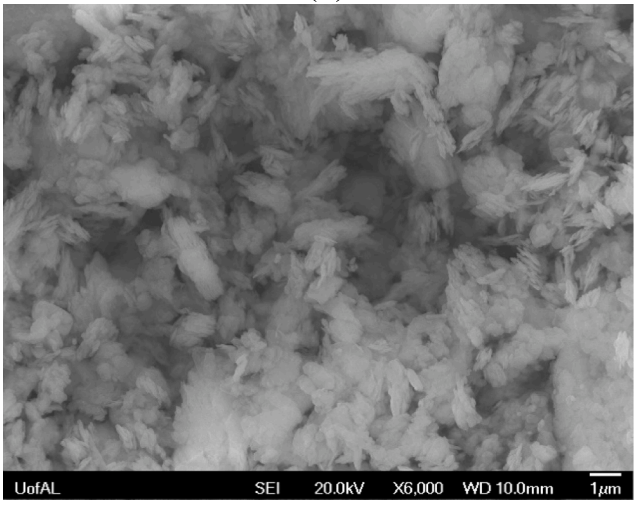

(d)

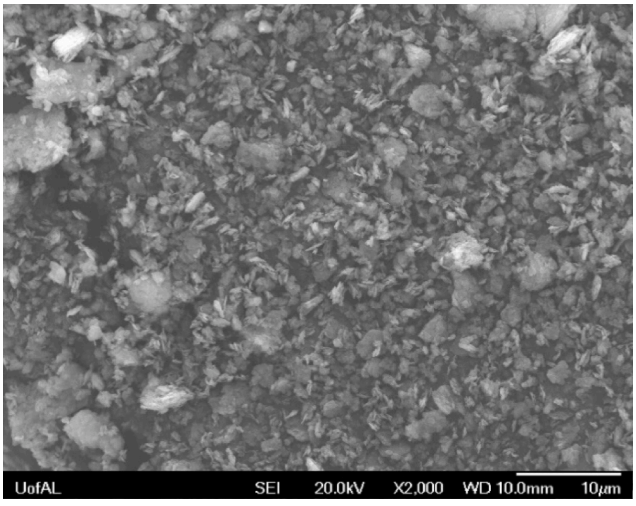

(e)

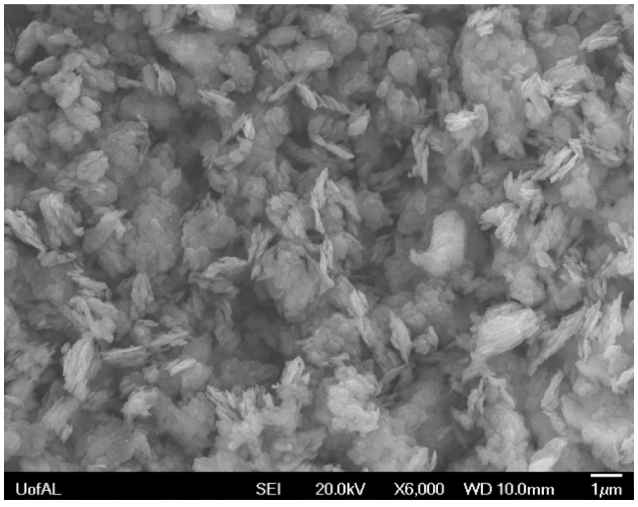

(f)

Fig. 3. Measurements of MK with and without TA dispersion: (a) FTIR spectra; (b) XRD pattern; (c) and (d) SEM image of MK without TA dispersion (e) and (f) SEM image MK with TA dispersion.

50 % and 95 % of the maximum load were selected to calculate the indentation stiffness. The volume fractions and the average mechanical properties were determined using the probability density function as the deconvolution method [24]. A Poisson ratio of 0.2 is adopted in the calculation of elastic modulus and packing density.

2.7. Compressive strength

A total of ten different mixes were prepared for compressive strength testing to evaluate the effect of TA as a dispersant for MK on the mechanical properties of produced cement mortars, as shown in Table 2. The Control mortar sample was produced without using MK. The MK blended cement mortars made without using TA dispersing are designated as XMK in the table, in which X refers to X% of cement substituted by MK. The MK blended mortar samples made with TA dispersing are referred to as XMKYTA in Table 2, where X and Y are the percentages of the cement substituted by the MK and the dosage (in 1 ‰) of the TA used to disperse the MK, respectively. For example, mortar sample 10MK2TA was produced by replacing 10 % cement with the same amount of MK dispersed by 2 ‰ TA (by weight of total cementitious materials). One extra group, 15MK2SP, was made with 15 % MK substitution dispersed by 2 ‰ superplasticizers (PCE). These mortar samples were cast into 50×100 mm cylinders and cured in standard conditions to determine their compressive strengths at different ages according to ASTM C39 [31].

3. Results and discussion

3.1. Characterization of TA dispersed MK

The strong interaction between TA and MK can be observed in Fig. 3 (a), which compares the FTIR spectrum of the MK with and without TA dispersion. The peaks at 1079 and 799 cm^{-1} correspond to the bending and asymmetric stretching mode of Si-O-Si bonds, respectively [32]. The vibration frequencies observed in pure TA at 1019, 1310, 1444, 1532, 1607, and 1697 cm^{-1} correspond to C—O asymmetric stretching, aromatic CH deformation, C-Carom stretching, ring vibrations, C═C stretching, and C═O stretching, respectively [33]. It can be seen that the last five bands were shifted to 1367, 1441, 1501, 1617, and 1698 cm^{-1}, respectively, confirming the presence of strong interaction between the TA and MK.

Fig. 3(b) presents the XRD patterns of MK with and without TA dispersion. The broad hump between the diffraction angle of 20° and 40° was attributed to the amorphous crystal structure in MK. The peaks of quartz were clearly higher for the TA dispersed MK. This is because partial aluminum can be dissolved in the TA solution (Eq. (3)), leading to a comparatively stronger peak of the quartz than that of the pristine MK. It was reported that certain organic acids, such as lactic acid, citric acid, and oxalic, can dissolve Al-silicates due to their metal chelating ability [34,35].

$$Al_2Si_2O_5(OH)_5 + 6H^+ \rightarrow 2Al^{3+} + 2H_4SiO_4 + H_2O \quad (3)$$

The morphologies of the MK before and after TA dispersion were obtained using SEM, as shown in Fig. 3(c-f). It can be seen that the TA dispersion reduced the aggregation of the MK in comparison with the pristine MK. It was reported that TA could interact with almost any surface due to abundant phenolic-OH groups [36]. In addition, MK itself has also proved to be an effective adsorbent for organic matter [37]. Hence, the existence of TA coating can make the MK particles negatively charged due to the phenolic-OH groups, increasing the stability of dispersed MK due to electrostatic repulsion. It was also observed in polyvinyl alcohol (PVA)-stabilized MK [38].

This observation was further confirmed by measuring the BET surface areas of the MK before and after TA dispersion, which are 19.69 m^2/g and 38.91 m^2/g, respectively. The 2 ‰ TA dispersion almost doubled the surface area compared to that of the pristine MK, agreeing with the observation obtained with SEM. The results of zeta potential tests also confirm that TA dispersion increases the stability of MK in an aqueous solution, as shown in Fig. 4. All these findings suggest that TA does have the ability to disperse the MK.

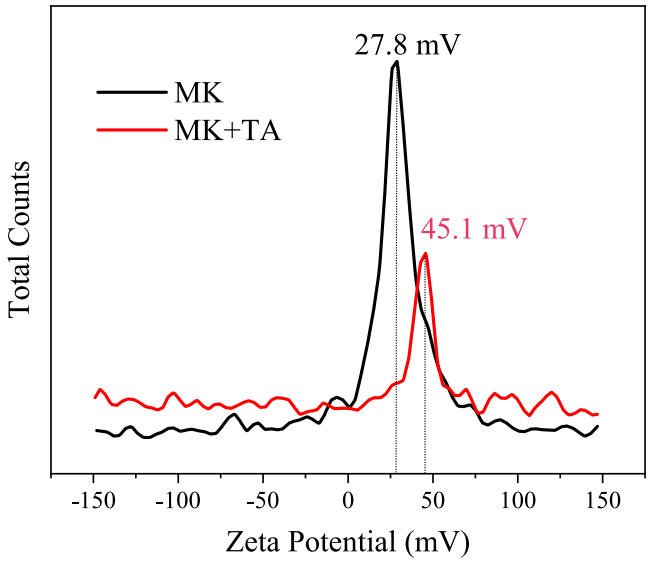

Fig. 4. Zeta potentials of MK with and without TA dispersion.

Table 3
Setting times of MK blended cement pastes.

Group	Initial Set (minutes)	Final Set (minutes)
Control	160	257
15MK	104	189
15MK2TA	251	353
15MK4TA	157	291
15MK6TA	80	184

3.2. Setting time, workability, and hydration evolution

Table 3 shows the effect of TA dispersion on the setting time of the produced cement paste. Both the initial and final setting time periods of the produced sample with the pristine MK were shorter than that of the Control group. This is because of the seeding effect of the highly reactive MK used in this study which has a particle size of around 1–2 μm. When 2 ‰ TA was used to disperse the MK, both setting time periods were significantly increased, as shown in Table 3, which can be attributed to the free TA in the TA dispersed MK slurry. Previous research indicated that the addition of TA itself can significantly retard the hydration of cement, similar to many other organic molecules [39]. In addition, TA has a strong ability to capture calcium ions [40] from fresh concrete to form calcium tannate nanoparticles, leading to insufficient calcium ions for hydration and pozzolanic reaction at early age. As a result, both initial and final setting time periods were significantly increased.

However, when the dosage of TA was increased further, both the initial and final setting time periods of produced cement paste were surprisingly reduced. When 6 ‰ TA is used to disperse MK, the initial setting time of the paste is only half of the control group. This is presumably due to the introduction of $Al(OH)_3$, which is known as a cement set accelerator [41]. As mentioned earlier, TA can be used to dissolve aluminum, and this dissolution rate is increased with a higher concentration of the TA [35]. When mixed with the cement, aluminum ions can be converted into $Al(OH)_3$ due to the increased pH value, accelerating the set of the paste. This effect of TA dispersion on the setting behavior of the produced paste provides us with a new way to adjust the setting

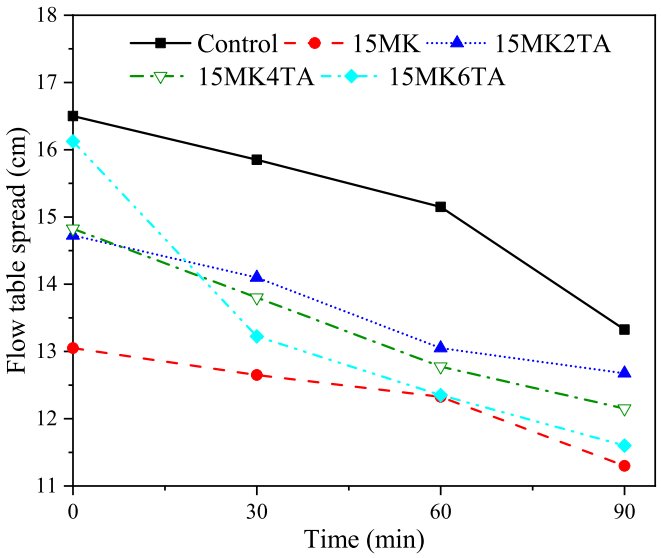

Fig. 5. Average spread diameter of the MK blended cement mortars after flow table test.

times of the cement paste to achieve the best performance.

The effect of TA dispersion can be clearly seen from the flowabilities of MK blended mortars with and without using TA dispersion, as shown in Fig. 5. Among all mortar samples tested, the one prepared with undispersed MK exhibits the lowest flowability. This verifies that MK can significantly reduce the workability of cement mortar due to its high surface area. The TA dispersion can partially recover this loss of workability induced by the MK. As revealed in Fig. 5, all mortars with TA dispersed MK have higher flowabilities in comparison with the ones without using TA, confirming the dispersion effect of the TA.

The effect of TA dispersion on the hydration of the MK blended cement was examined by the isothermal calorimetry, and the results are shown in Fig. 6. The addition of the pristine MK slightly accelerated the hydration of the cement paste at early age due to the high surface area of the MK. Similar results have been widely reported in the literature [42]. Once TA was added, the released hydration heat was enhanced in the first 3.5 h, as shown in Fig. 6(c). This is because the dissolution of the cement clinker was also enhanced by the TA at early age through forming TA-calcium chelation, similar to the dissolution of the MK in the TA solution. The formation of TA-calcium chelation not only consumed the calcium ions in the fresh paste but also inhibited the precipitation of the hydration products through its dispersion ability, leading to a severe retarding effect on the hydration of the cement after 3.5 h. The peak corresponding to C_3S hydration was delayed to almost 24 h, as revealed by Fig. 6(a), which is in agreement with the setting time of those pastes shown in Table 3.

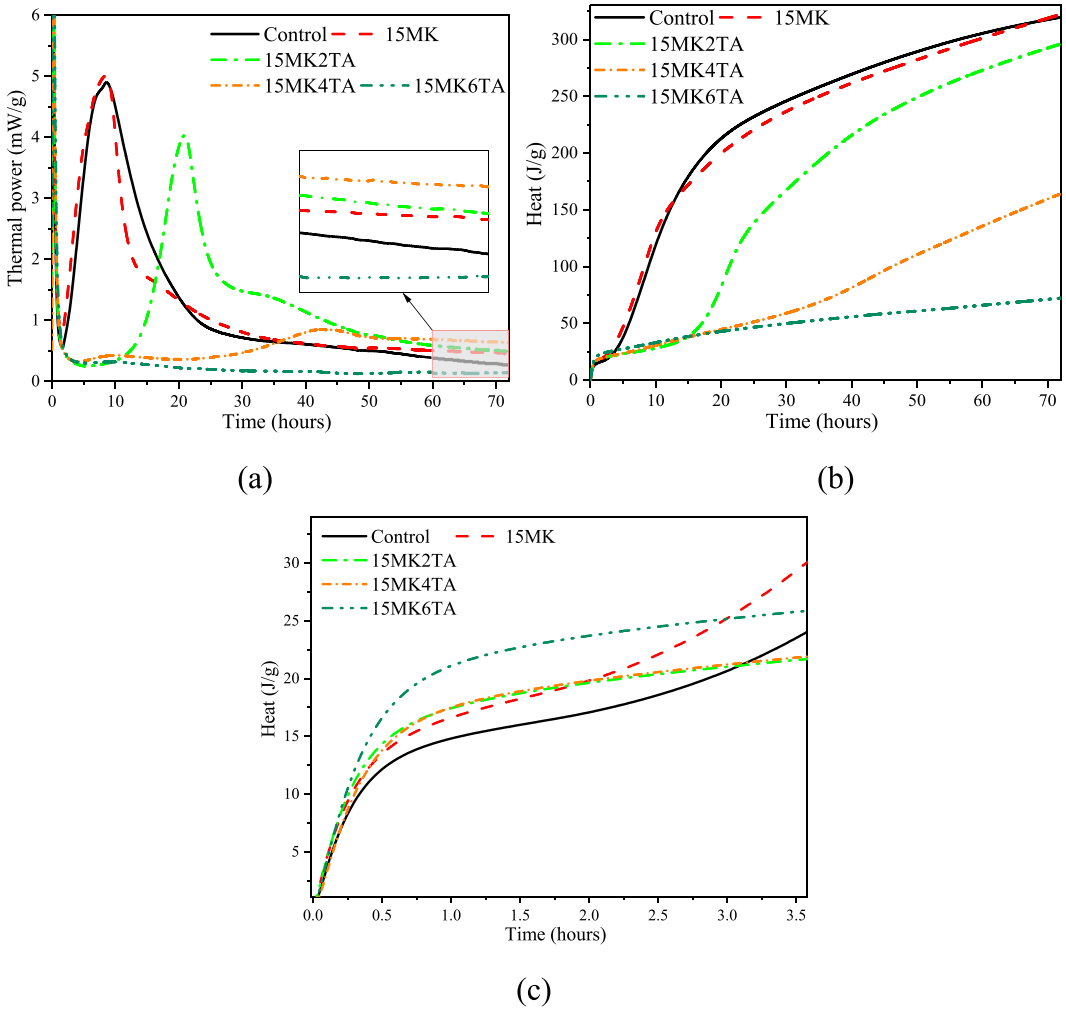

Fig. 6. Isothermal calorimetry curves of MK blended pastes produced with different methods: (a) Thermal power; (b) Accumulated released hydration heat for 72 h; (c) Accumulated released hydration heat for the first 3.5 h.

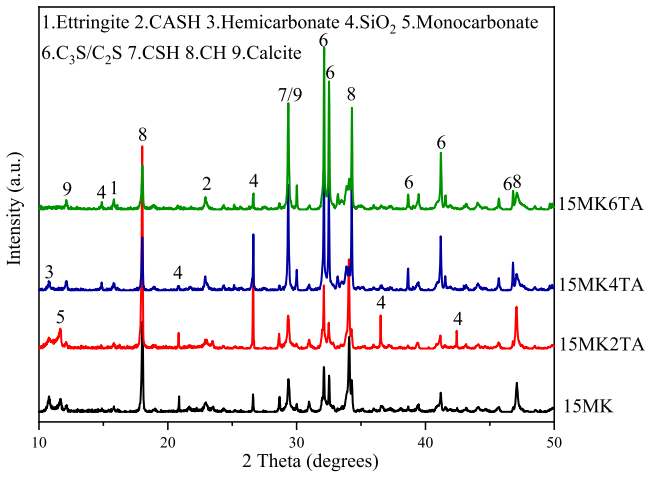

(a)

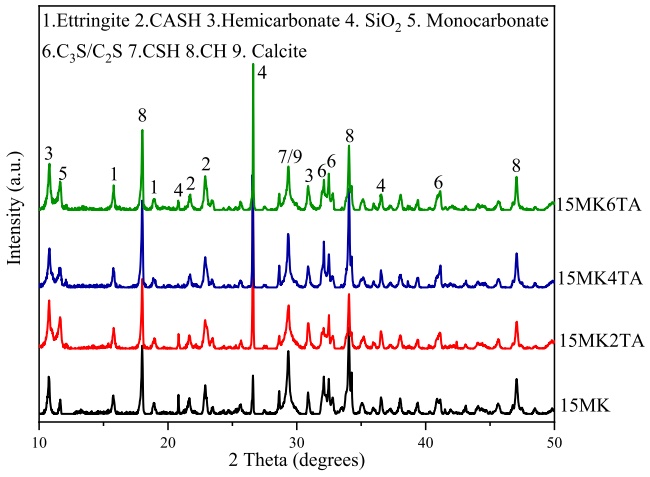

(b)

Fig. 7. XRD patterns of cement paste produced with the TA dispersed MK at: (a) 3 days; (b) 28 days.

At the late age (after 60 h), the hydration rates of 15MK2TA and 15MK4TA samples surpassed that of the control group, indicating that TA dispersion has a delayed acceleration effect, as shown in the enlarged area of Fig. 6(a). This is similar to Juenger and Jennings's finding of the retarding effect of sugar on cement hydration [43]. In the case of 15MK6TA, the cement hydration remained dormant at the end of 72 h, suggesting a more severe retarding effect can be induced by more TA.

3.3. Hydration products

The effect of TA dispersion on the hydration products is revealed by the XRD spectra shown in Fig. 7. Typical hydration products such as CH, C—S—H, C-A—S—H, and ettringite are marked on these spectra. No new mineral was detected by these spectra. It can be seen that the peaks of C_2S and C_3S of the samples with TA dispersed MK are higher than those of the ones without TA dispersion at early age, as shown in Fig. 7(a), which is mainly due to the retarding effect of the TA. The intensity of these peaks increases with the content of TA used for dispersing, indicating that retarding effect is more severe with more TA added. After hydration of 28 days, the intensities of the peaks of C_2S and C_3S of all paste samples converge, as shown in Fig. 7(b), suggesting that the retarding effect of TA diminished at this age, and all pastes have a similar degree of hydration.

It is interesting to note that the intensity of quartz increased with the content of the TA used to disperse the MK. This indicates that a higher degree of reaction of the MK is achieved by using more TA [44], which is in agreement with Fig. 3. Therefore, the reaction between the MK and hydration products of cement is promoted by the TA dispersion at late age, even though the early age reaction is retarded by the TA.

3.4. Microstructure

Fig. 8 shows the representative microstructures of the MK blended cement pastes produced with and without TA dispersion. It can be found that cement paste with TA dispersed MK (15MK2TA) has a much denser microstructure compared with the one prepared with pristine MK, as revealed by Fig. 8(a–d). Much more micro-pores or cracks can be observed on the 15MK specimen shown in Fig. 8(a and b), clearly demonstrating the necessity of dispersing MK. Numerous nanoparticles with a size of around 10 to 20 nm were found in this specimen prepared with TA dispersed MK, as shown in Fig. 8(e and f). The previous study suggested [25] that these nanoparticles were in-situ produced by complexation between the calcium ions released from the cement and TA. It is anticipated that the presence of these nanoparticles can improve the particle packing of the hydrated cement, leading to significant improvement in the mechanical properties of the produced mortars.

The MIP tests of cement pastes at 28 days were carried out to confirm the observation obtained by SEM, and the results are shown in Fig. 9 and Table 5. The dispersion effect of TA can be clearly seen in Fig. 9, which shows the large capillary pores with the size of around 1 μm in 15MK paste were drastically reduced and refined by the TA dispersion. There large capillary pores were also reduced by using the superplasticizer (PCE), suggesting that the PCE can also improve the dispersion of the MK. Nevertheless, more reduction of the total porosity of the MK blended cement paste was achieved by using TA. The major difference between using TA and PCE is that interhydrate pores (with a size smaller than 20 nm) and gel pores were drastically reduced by using TA in comparison with the one using PCE. This suggests that TA dispersion has the potential to densify the hydration products, mainly C—S—H. One possible reason is that the large amount of in-situ produced nanoparticles shown in Fig. 9(c) may function as nanofillers to fill the small capillary pores. Another possible reason is the DOPA-like ability of TA to bind to various hydration products, providing extra adhesion to improve the packing density of the hydration products. This reduction in small capillary pores can not only increase the strength of concrete but also lead to improvements in drying shrinkage and creep performance of the concrete since these properties of concrete are controlled by nanopores with a size smaller than 30 nm [45]. This higher packing density of hydration products consumes more solid hydration products. As a result, more capillary pores with size near 100 nm were generated in the TA dispersed sample, as indicated by the higher peak of 15MK2TA in Fig. 9 (a).

Changes in pore structure inevitably affected the mechanical properties of the hydration products, as revealed by the elastic modulus of the MK blended cement pastes obtained by nanoindentation shown in Fig. 10. This figure presents deconvolution results to determine the elastic modulus and packing density for MK blended cement paste with and without TA dispersion. In these figures, π, μ and σ represent the volume fraction of the phase, mean value (in GPa), and standard deviation (in GPa), respectively. As shown in Fig. 10(a), three C—S—H phases, low-density (LD) C—S—H, high density (HD) C—S—H, and CH/C—S—H [46], are identified in the MK blended cement paste without using TA dispersion. Based on Tennis and Jennings' theory [47], LD and HD C—S—H are made of the same nanosized building blocks (4–5 nm). After TA was used to disperse the MK, the LD C—S—H phase disappeared, and the volume fractions of HD C—S—H and CH/C—S—H were increased from 0.65, 0.13 to 0.77 and 0.23, respectively. Fig. 10(c and d) show the packing densities of the pastes without using TA and with TA. Clearly, dispersing MK with TA significantly densified the

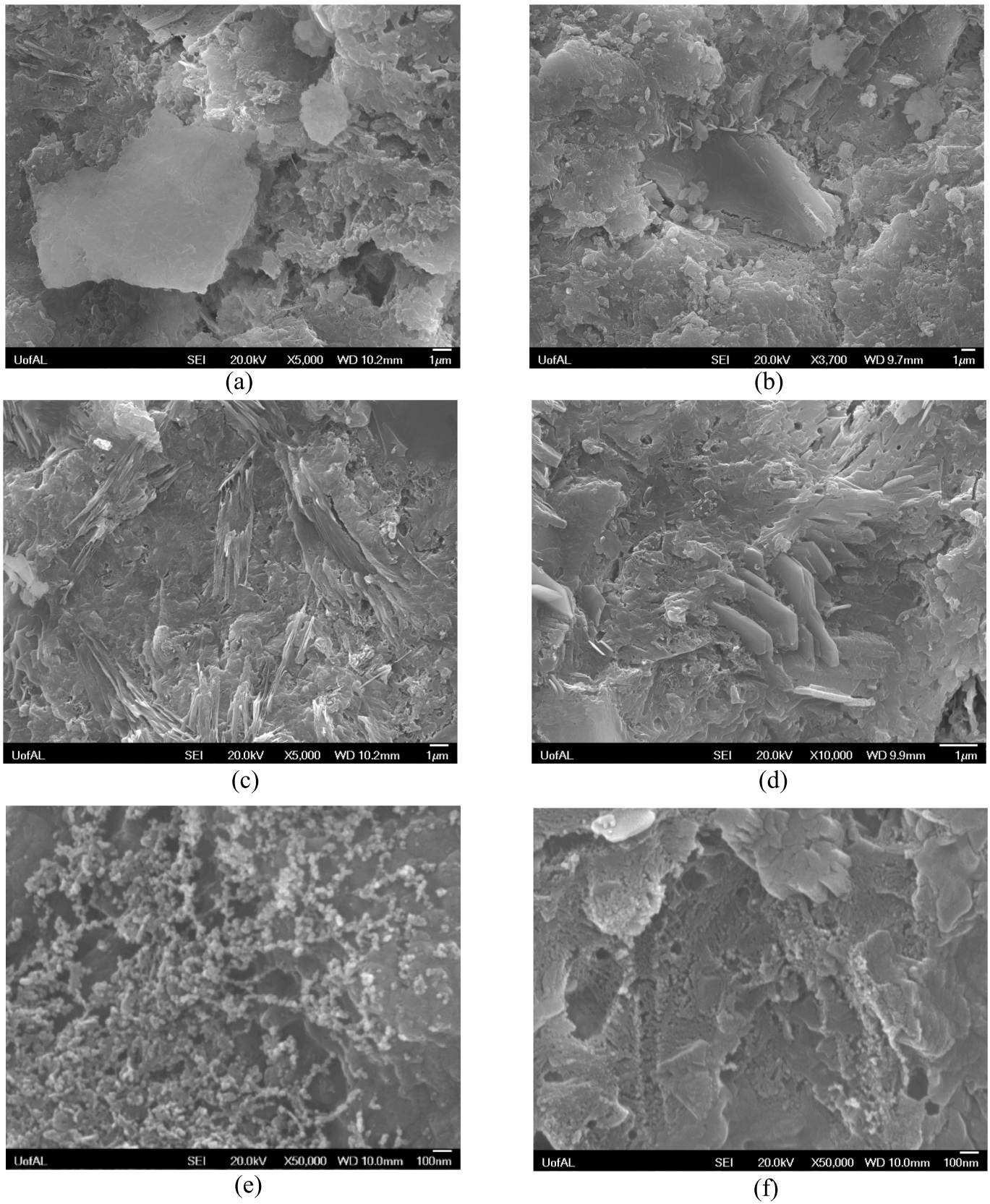

Fig. 8. SEM images of MK blended cement pastes at 28 days: (a) and (b)15MK; (c) and (d) 15MK2TA; (e) and (f) nanoparticles in 15MK2TA.

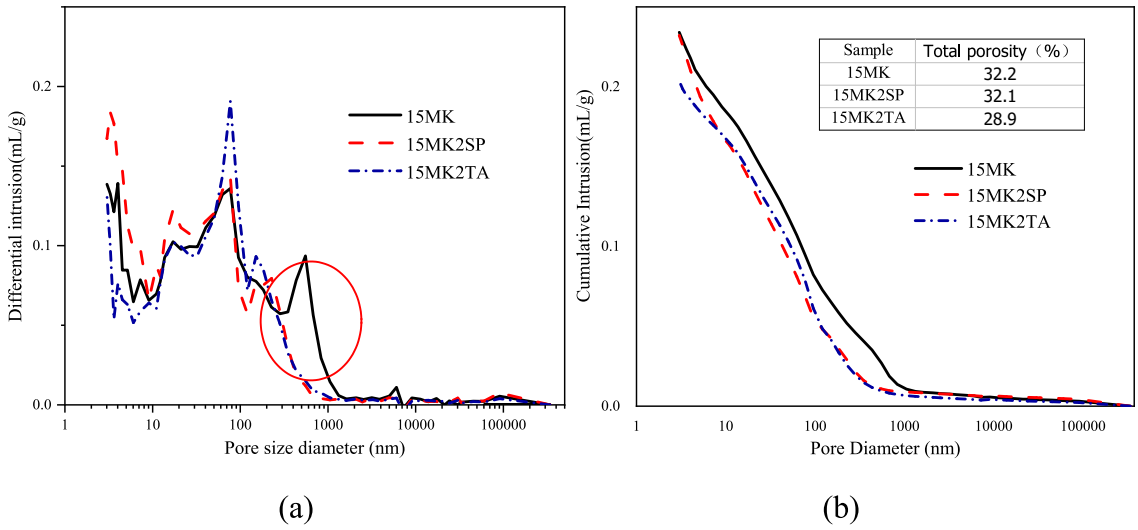

Fig. 9. Pore structure of cement pastes with and without using TA dispersed MK at 28 days: (a) differential pore-size distribution;(b) cumulative pore volume.

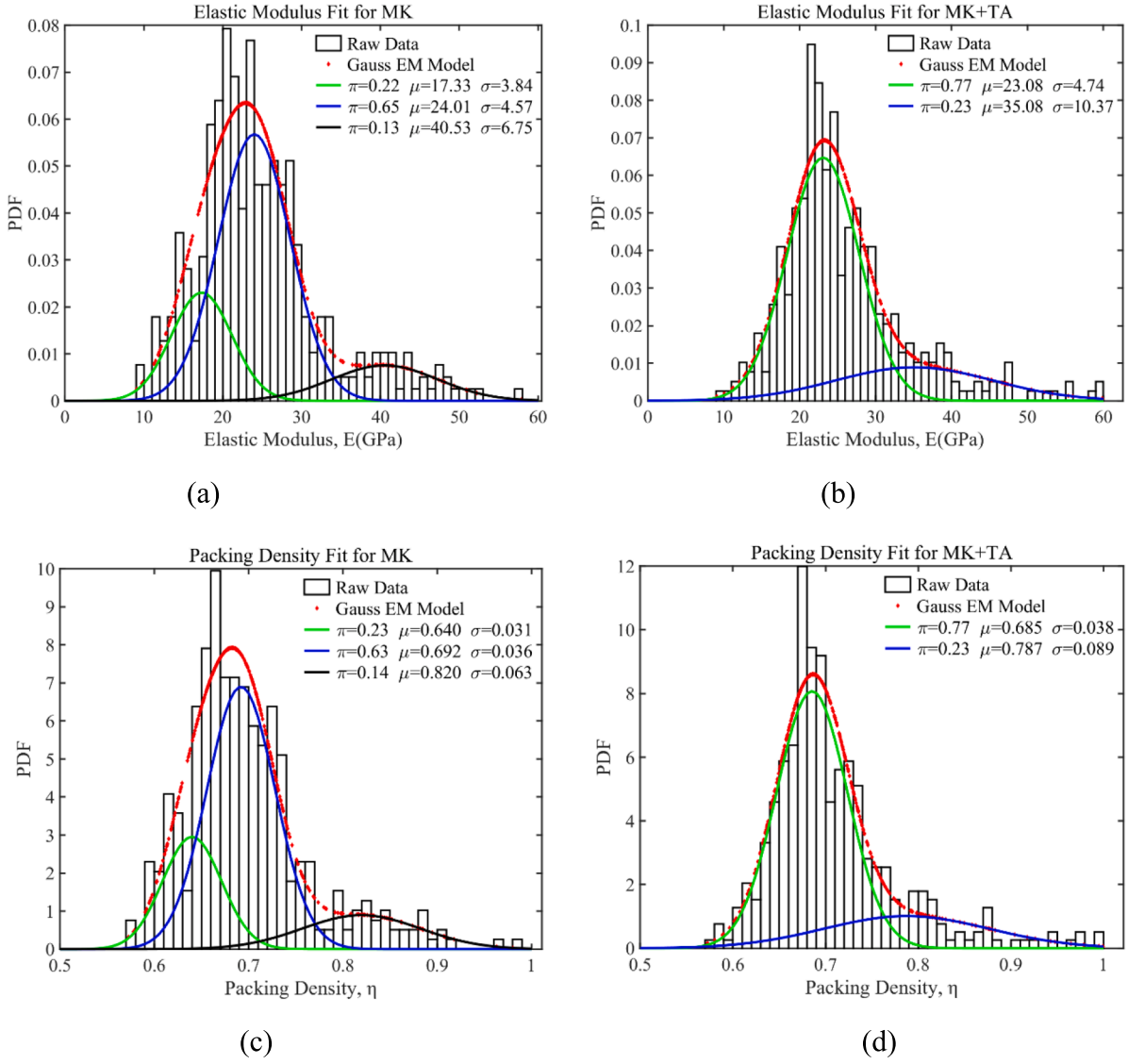

Fig. 10. Deconvolution results of elastic modulus and packing density obtained from the pastes: (a) and (c) 15MK; (b) and (d) 15MK2TA.

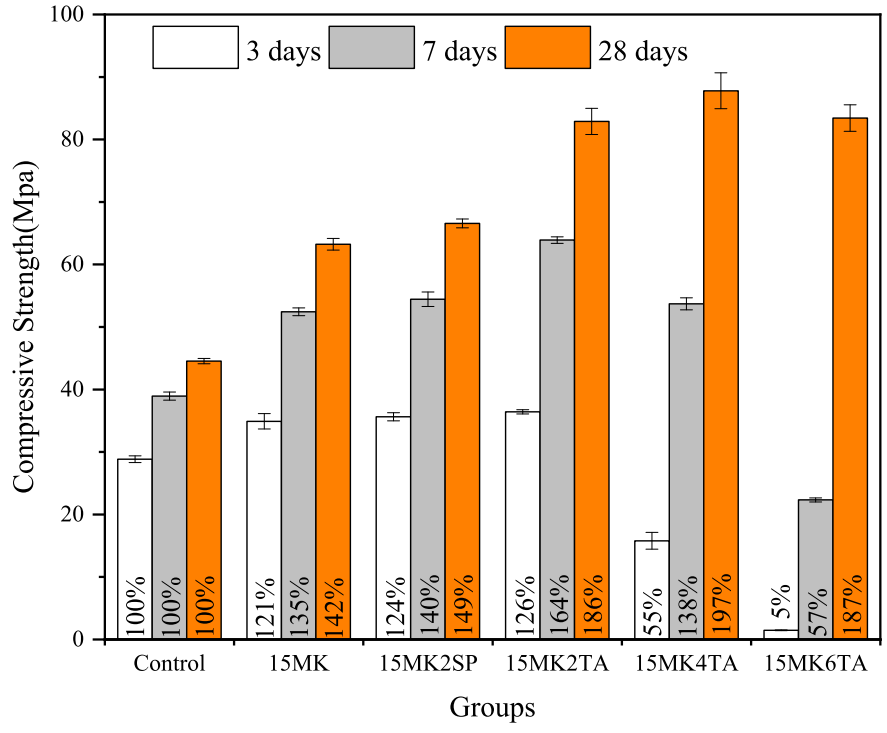

(a)

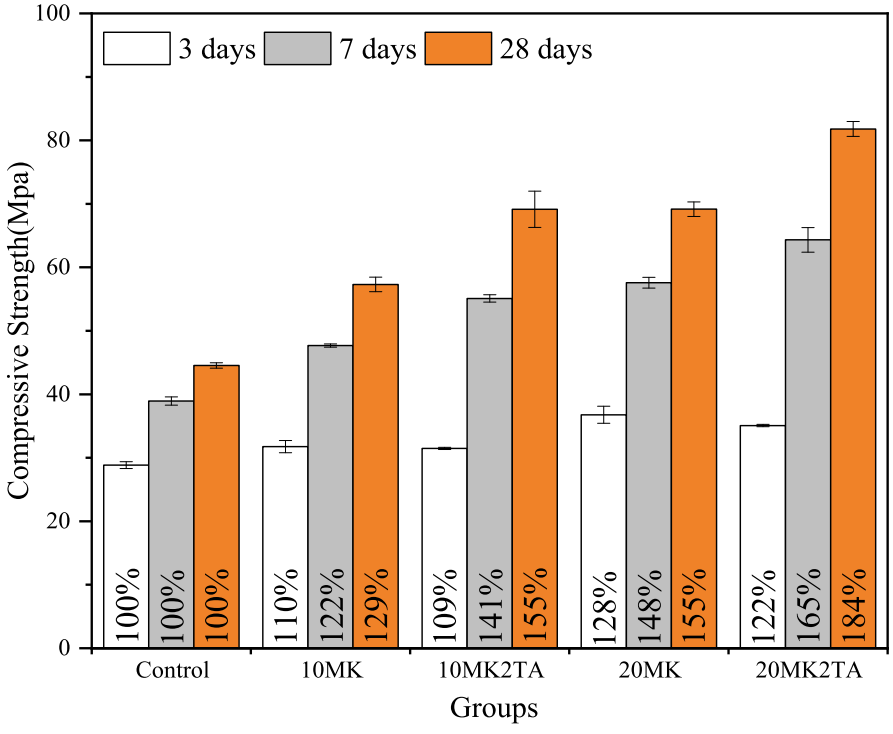

(b)

Fig. 11. Compressive strength of cement mortar prepared with different percentages of TA dispersed MK: (a)15%; (b) 10% and 20%.

produced hydration phases. This densifying effect results from reduced interhydrate and gel pores induced by the TA, as shown in Fig. 9.

3.5. Compressive strength

MIP and nanoindentation results (Figs. 9 and 10) suggest that TA dispersion has a profound effect on the pore structure and micro-mechanical properties of the hydration phases. Consequently, the macromechanical properties of produced cement mortars are anticipated to be significantly improved by the TA dispersed MK. Fig. 11 compares the compressive strengths of cement mortars with the mix design detailed in Table 2. Replacing 15 % cement with MK improves the compressive strength of the mortar at 3 days, 7 days, and 28 days by 21 %, 35 %, and 42 %, respectively. This observation agrees with existing studies, which established that MK could significantly improve the performance of produced cement concrete [5–7]. When TA was used to disperse the MK, all these strengths were drastically improved compared to the one prepared with pristine MK. For example, by using 2 ‰ TA (by the weight of total cementitious materials) to disperse MK, the compressive strengths of the mortar at 3 days, 7 days, and 28 days were improved by 26 %, 64 %, and 86 %, respectively, confirming the speculation that the densified microstructure can significantly enhance the compressive strength. This strength enhancement cannot be achieved by dispersing MK with 2 ‰ of superplasticizer. Using superplasticizer is slightly better than using pristine MK but significantly lower than those prepared using TA dispersed MK.

Increasing the content of TA to 4 ‰ led to a 97 % increase in the compressive strength of the mortar at 28 days. There is a 45 % strength reduction in the cement prepared with 6 ‰ TA dispersed MK. However, higher compressive strength at late age was also achieved compared to the one prepared with pure MK. Even though the use of TA can retard the cement hydration significantly, the compressive strength of 15MK4TA reaches almost 90 MPa at 28 days, which is already significantly higher than the standard of high-performance concrete. It should be mentioned that all the mortars prepared in the compressive strength test employed water to binder ratio of 0.5, which means the efficiency of the binding materials were significantly enhanced, making it a low-CO_2 high-performance cement concrete.

Fig. 11(b) illustrates the effectiveness of the TA dispersion for a different amount of MK replacement. When replacing 10 % of cement with MK, the compressive strengths of the mortar at 3 days, 7 days, and 28 days were improved by 10 %, 22 %, and 29 %, respectively. After dispersing the MK with 2 ‰ TA, these compressive strengths were enhanced by 9 %, 41 %, and 55 %, respectively. When MK content was increased to 20 %, the compressive strengths of the mortar at 3 days, 7 days, and 28 days were improved by 28 %, 48 %, and 55 %, respectively. In this case, the achieved improvement in the compressive strength of the mortar is much more significant than using just 10 % and 15 % MK. Nevertheless, this improvement can be further enhanced by dispersing the MK with 2 ‰ TA. As shown in Fig. 11(b), the compressive strengths at these three ages were improved by 22 %, 65 %, and 84 %, respectively.

It is of great importance to achieve higher strength without using more cement. In this way, the total amount of concrete required for a specific construction process is reduced, which not only saves a large number of natural resources (aggregates), but also reduces the total carbon emission of the construction. It was reported that the CO_2 emission per cubic meter of concrete is linear to the square root of its compressive strength f_c' [48]. Considering 86 % improvement of strength achieved by 15MK2TA at 28 days over the control mortar, the present study can reduce the CO_2 emission of the mortar with compressive strength of $1.86f_c$' to that of mortar with compressive strength of $1.0f_c$', equivalent to reducing the CO_2 emission of the mortar by at least 27 % from the perspective of strength.

4. Conclusions

This study proposes an eco-friendly admixture to disperse MK in cement mortar to achieve much better performance. The admixture adopted in this study is a plant-derived polyphenol, tannic acid, which is inspired by the extraordinary ability of mussels to adhere to various surfaces. With a similar chemical structure to the DOPA protein of mussels, TA can be adsorbed on the surface of the MK particles to form a layer of TA on the surface of the MK particle, which not only reduces the aggregation/agglomeration of the MK but also results in better workability of the fresh mortar. More importantly, TA can significantly reduce the nanopores with sizes less than 30 nm. This suggests that the hydration products such as C—S—H are densified by the presence of TA, which cannot be achieved by using a traditional superplasticizer(PCE) for dispersion. The nanoindentation test confirms this finding, revealing that TA dispersion densifies the LD C—S—H into HD C—S—H. As a result, the compressive strength of the produced mortar has been drastically improved, as evidenced by nearly doubled compressive strength at 28 days achieved by the mortars using 15 %MK dispersed by 0.4 %TA, exhibiting a great potential of reducing the carbon footprint of OPC-based materials.

Although extensive works have been carried out to enhance the sustainability of concretes, little work has been carried out to improve the sustainability of the chemical admixtures. This study suggests that natural products such as TA have the potential to replace the traditional, petroleum-based chemical admixtures for concrete. Compared with traditional admixtures, these admixtures enjoy many advantages in sustainability, including being renewable, low-carbon or even carbon-negative, non-toxic, and locally available.

CRediT authorship contribution statement

Xin Qian: Methodology, Investigation, Visualization, Writing – original draft. **Mengxiao Li:** Investigation. **Jialai Wang:** Conceptualization, Funding acquisition, Supervision, Writing – review & editing. **Liang Wang:** Investigation. **Peiyuan Chen:** Investigation. **Yi Fang:** Methodology, Investigation, Writing – review & editing. **Xiaodong Wang:** . **Fan Yang:** Investigation.

Declaration of Competing Interest

The authors declare that they have no known competing financial interests or personal relationships that could have appeared to influence the work reported in this paper.

Data availability

Data will be made available on request.

Acknowledgements

The financial supports from the U.S. National Science Foundation (CMMI#1563551 and CMMI# 1761672), the National Natural Science Foundation of China (51908418), and the Fundamental Research Funds for the Central Universities at Tongji University are highly appreciated. Any Opinions, findings and conclusions or recommendations expressed in this material are those of the author(s) and do not necessarily reflect those of the National Science Foundation.

References

[1] B. Lothenbach, K. Scrivener, R.D. Hooton, Supplementary cementitious materials, Cem. Concr. Res. 41 (2011) 1244–1256, https://doi.org/10.1016/j.cemconres.2010.12.001.

[2] M.C.G. Juenger, R. Siddique, Recent advances in understanding the role of supplementary cementitious materials in concrete, Cem. Concr. Res. 78 (2015) 71–80.

[3] A.M. Rashad, Metakaolin as cementitious material: History, scours, production and composition-A comprehensive overview, Constr. Build. Mater. 41 (2013) 303–318, https://doi.org/10.1016/j.conbuildmat.2012.12.001.
[4] Z. Li, Z. Ding, Property improvement of Portland cement by incorporating with metakaolin and slag, Cem. Concr. Res. 33 (2003) 579–584, https://doi.org/10.1016/S0008-8846(02)01025-6.
[5] R. Siddique, J. Klaus, Influence of metakaolin on the properties of mortar and concrete: A review, Appl. Clay Sci. 43 (2009) 392–400, https://doi.org/10.1016/j.clay.2008.11.007.
[6] P. Dinakar, P.K. Sahoo, G. Sriram, Effect of Metakaolin Content on the Properties of High Strength Concrete, Int. J. Concr. Struct. Mater. 7 (2013) 215–223, https://doi.org/10.1007/s40069-013-0045-0.
[7] H.S. Al-alaily, A.A.A. Hassan, Refined statistical modeling for chloride permeability and strength of concrete containing metakaolin, Constr. Build. Mater. 114 (2016) 564–579.
[8] K.A. Gruber, T. Ramlochan, A. Boddy, R.D. Hooton, M.D.A. Thomas, Increasing concrete durability with high-reactivity metakaolin, Cem. Concr. Compos. 23 (6) (2001) 479–484.
[9] N.M. Al-Akhras, Durability of metakaolin concrete to sulfate attack, Cem. Concr. Res. 36 (9) (2006) 1727–1734.
[10] L. Shi, J. Liu, J. Liu, Effect of polymer coating on the properties of surface layer concrete, in, Procedia Eng. (2012) 291–300, https://doi.org/10.1016/j.proeng.2011.12.455.
[11] H. Paiva, A. Velosa, P. Cachim, V.M. Ferreira, Effect of metakaolin dispersion on the fresh and hardened state properties of concrete, Cem. Concr. Res. 42 (2012) 607–612, https://doi.org/10.1016/j.cemconres.2012.01.005.
[12] A.T. Bakera, M.G. Alexander, Use of metakaolin as a supplementary cementitious material in concrete, with a focus on durability properties, RILEM Tech. Lett. 4 (2019), https://doi.org/10.21809/rilemtechlett.2019.94.
[13] A.E. Hagerman, K.M. Riedl, G.A. Jones, K.N. Sovik, N.T. Ritchard, P.W. Hartzfeld, T.L. Riechel, High Molecular Weight Plant Polyphenolics (Tannins) as Biological Antioxidants, J. Agric. Food Chem. 46 (1998) 1887–1892, https://doi.org/10.1021/jf970975b.
[14] X. Fei, W. Wei, F. Zhao, Y. Zhu, J. Luo, M. Chen, X. Liu, Efficient Toughening of Epoxy-Anhydride Thermosets with a Biobased Tannic Acid Derivative, ACS Sustain. Chem. Eng. 5 (2017) 596–603, https://doi.org/10.1021/acssuschemeng.6b01967.
[15] J. Liu, H. Chen, Z. Xu, S. Zheng, M. Xue, Adsorption of tannic acid from aqueous solution by aminopropyl functionalized SBA-15, Desalin. Water Treat. 56 (2015) 475–484, https://doi.org/10.1080/19443994.2014.940394.
[16] A. Schieber, F. Stintzing, R. Carle, By-products of plant food processing as a source of functional compounds — recent developments, Trends Food Sci. Technol. 12 (2001) 401–413, https://doi.org/10.1016/S0924-2244(02)00012-2.
[17] J. Guo, Y. Ping, H. Ejima, K. Alt, M. Meissner, J.J. Richardson, Y. Yan, K. Peter, D. Von Elverfeldt, C.E. Hagemeyer, F. Caruso, Engineering multifunctional capsules through the assembly of metal-phenolic networks, Angew. Chemie – Int. Ed. 53 (2014) 5546–5551, https://doi.org/10.1002/anie.201311136.
[18] J.H. Waite, Nature's underwater adhesive specialist, Int. J. Adhes. Adhes. 7 (1987) 9–14, https://doi.org/10.1016/0143-7496(87)90048-0.
[19] J.H. Waite, M.L. Tanzer, Polyphenolic Substance of Mytilus edulis : Novel Adhesive Containing L-Dopa and Hydroxyproline, Science 212 (4498) (1981) 1038–1040.
[20] E. Faure, C. Falentin-Daudré, C. Jérôme, J. Lyskawa, D. Fournier, P. Woisel, C. Detrembleur, Catechols as versatile platforms in polymer chemistry, Prog. Polym. Sci. 38 (2013) 236–270, https://doi.org/10.1016/j.progpolymsci.2012.06.004.
[21] H.J. Cha, D.S. Hwang, S. Lim, Development of bioadhesives from marine mussels, Biotechnol. J. 3 (2008) 631–638, https://doi.org/10.1002/biot.200700258.
[22] J.J. Wilker, The iron-fortified adhesive system of marine mussels, Angew. Chemie – Int. Ed. 49 (2010) 8076–8078, https://doi.org/10.1002/anie.201003171.
[23] H. Lee, N.F. Scherer, P.B. Messersmith, Single-molecule mechanics of mussel adhesion, Proc. Natl. Acad. Sci. 103 (2006) 12999–13003, https://doi.org/10.1073/pnas.0605552103.
[24] Y. Fang, J. Wang, H. Ma, L. Wang, X. Qian, P. Qiao, Performance enhancement of silica fume blended mortars using bio-functionalized nano-silica, Constr. Build. Mater. 312 (2021), 125467, https://doi.org/10.1016/j.conbuildmat.2021.125467.
[25] Y.i. Fang, J. Wang, X. Qian, L. Wang, P. Chen, P. Qiao, A renewable admixture to enhance the performance of cement mortars through a pre-hydration method, J. Clean. Prod. 332 (2022) 130095.
[26] M.A. Rahim, H. Ejima, K.L. Cho, K. Kempe, M. Müllner, J.P. Best, F. Caruso, Coordination-driven multistep assembly of metal-polyphenol films and capsules, Chem. Mater. 26 (2014) 1645–1653, https://doi.org/10.1021/cm403903m.
[27] ASTM, C191−13:Standard Test Methods for Time of Setting of Hydraulic Cement by Vicat Needle, West Conshohocken, PA, 2013.
[28] Astm, C1437–01: Standard Test Method for Flow of Hydraulic Cement Mortar, Standard. (2001) 7–8, https://doi.org/10.1520/C1437-13.2.
[29] Astm, C1679–14: Measuring Hydration Kinetics of Hydraulic Cementitious Mixtures Using, Isothermal Calorimetry (2014), https://doi.org/10.1520/C1679-14.
[30] ASTM, C1702-17: Standard Practice for Measurement of Heat of Hydration of Hydraulic Cementitious Materials Using Isothermal Conduction Calorimetry, West Conshohocken, PA, 2017. https://doi.org/10.1520/C1702-17.
[31] ASTM, C39/C39M-21:Standard Test Method for Compressive Strength of Cylindrical Concrete Specimens, West Conshohocken, PA, 2021.
[32] B. Ilić, V. Radonjanin, M. Malešev, M. Zdujić, A. Mitrović, Effects of mechanical and thermal activation on pozzolanic activity of kaolin containing mica, Appl. Clay Sci. 123 (2016) 173–181, https://doi.org/10.1016/j.clay.2016.01.029.
[33] A. Ricci, K.J. Olejar, G.P. Parpinello, P.A. Kilmartin, A. Versari, Application of Fourier transform infrared (FTIR) spectroscopy in the characterization of tannins, Appl. Spectrosc. Rev. 50 (2015) 407–442, https://doi.org/10.1080/05704928.2014.1000461.
[34] J. Cama, J. Ganor, The effects of organic acids on the dissolution of silicate minerals: A case study of oxalate catalysis of kaolinite dissolution, Geochim. Cosmochim. Acta. 70 (2006) 2191–2209, https://doi.org/10.1016/j.gca.2006.01.028.
[35] D. Karbalaei Saleh, H. Abdollahi, M. Noaparast, A. Fallah Nosratabad, Dissolution of aluminium from metakaolin with oxalic, citric and lactic acids, Clay Miner. 54 (2019) 209–217, https://doi.org/10.1180/clm.2019.28.
[36] X. Zhang, M. Liu, X. Zhang, F. Deng, C. Zhou, J. Hui, W. Liu, Y. Wei, Interaction of tannic acid with carbon nanotubes: Enhancement of dispersibility and biocompatibility, Toxicol. Res. (Camb) 4 (2015) 160–168, https://doi.org/10.1039/c4tx00066h.
[37] M.Y. Chang, R.S. Juang, Adsorption of tannic acid, humic acid, and dyes from water using the composite of chitosan and activated clay, J. Colloid Interface Sci. 278 (2004) 18–25, https://doi.org/10.1016/j.jcis.2004.05.029.
[38] N.P. Lukuttsova, A.A. Pykin, Stability of Nanodisperse Additives Based on Metakaolin, Glas. Ceram. (English Transl. Steklo i Keramika). 71 (2015) 383–386, https://doi.org/10.1007/s10717-015-9693-7.
[39] L. Wang, J. Wang, X. Qian, Y. Fang, P. Chen, A. Tuinukuafe, Tea stain-inspired treatment for fine recycled concrete aggregates, Constr. Build. Mater. 262 (2020), 120027, https://doi.org/10.1016/j.conbuildmat.2020.120027.
[40] S.W. Ju, E. Prajatelistia, S.H. Jun, D.S. Hwang, J.S. Ahn, N.D. Sanandiya, Aesthetically improved and efficient tannin-metal chelates for the treatment of dentinal hypersensitivity, RSC Adv. 7 (2017) 87–94, https://doi.org/10.1039/c6ra24745h.
[41] A.S. Brykov, A.S. Vasil'ev, M.V. Mokeev, Hydration of portland cement in the presence of aluminum-containing setting accelerators, Russ. J. Appl. Chem. 86 (6) (2013) 793–801.
[42] F. Lagier, K.E. Kurtis, Influence of Portland cement composition on early age reactions with metakaolin, Cem. Concr. Res. 37 (2007) 1411–1417, https://doi.org/10.1016/j.cemconres.2007.07.002.
[43] M.C. Garci Juenger, H.M. Jennings, New insights into the effects of sugar on the hydration and microstructure of cement pastes, Cem. Concr. Res. 32 (2002) 393–399, https://doi.org/10.1016/S0008-8846(01)00689-5.
[44] S. Scherb, M. Köberl, N. Beuntner, K.-C. Thienel, J. Neubauer, Reactivity of metakaolin in alkaline environment: Correlation of results from dissolution experiments with XRD quantifications, Materials (Basel). 13 (10) (2020) 2214.
[45] H.M. Jennings, J.W. Bullard, J.J. Thomas, J.E. Andrade, J.J. Chen, G.W. Scherer, Characterization and Modeling of Pores and Surfaces in Cement Paste, J. Adv. Concr. Technol. 6 (2008) 5–29, https://doi.org/10.3151/jact.6.5.
[46] J.J. Chen, L. Sorelli, M. Vandamme, F.J. Ulm, G. Chanvillard, A coupled nanoindentation/SEM-EDS study on low water/cement ratio portland cement paste: Evidence for C-S-H/Ca(OH)2 nanocomposites, J. Am. Ceram. Soc. 93 (2010), https://doi.org/10.1111/j.1551-2916.2009.03599.x.
[47] P.D. Tennis, H.M. Jennings, Model for two types of calcium silicate hydrate in the microstructure of Portland cement pastes, Cem. Concr. Res. 30 (2000) 855–863, https://doi.org/10.1016/S0008-8846(00)00257-X.
[48] G. Habert, N. Roussel, Study of two concrete mix-design strategies to reach carbon mitigation objectives, Cem. Concr. Compos. 31 (6) (2009) 397–402.